Contents lists available at Science-Gate

International Journal of Advanced and Applied Sciences

Journal homepage: http://www.science-gate.com/IJAAS.html

An automated approach for prostate cancer detection using CGAN data augmentation with a weighted ensemble of transfer learning models

Raafat M. Munshi *

Department of Medical Laboratory Technology (MLT), Faculty of Applied Medical Sciences, King Abdulaziz University, Rabigh, Saudi Arabia

ARTICLE INFO

Article history:
Received 19 June 2025
Received in revised form
16 October 2025
Accepted 16 November 2025

Keywords:
Prostate cancer
Deep learning
Generative adversarial network
Ensemble model
Medical imaging

ABSTRACT

Prostate cancer is one of the most common and lethal cancers among men worldwide, often developing without symptoms or with only minor signs, which makes early detection difficult. This study introduces a novel deep learning framework that integrates a Conditional Generative Adversarial Network (CGAN) with a weighted ensemble model consisting of ResNet (15%), Xception (50%), and Inception (35%). The model was trained and evaluated on the publicly available PROSTATEx image dataset, with performance measured using accuracy, precision, recall, and F1-score. The proposed weighted ensemble achieved 98.25% accuracy, 96.75% precision, 97.58% recall, and 96.65% F1-score, outperforming the soft voting ensemble, which obtained 95% accuracy, 92% precision, 94% recall, and 93% F1-score. Comparative analysis with state-of-the-art methods and cross-validation further confirmed the robustness of the proposed approach. These findings suggest that integrating CGAN with a weighted ensemble significantly enhances prostate cancer detection and holds strong potential for clinical application in early diagnosis and patient management.

1. Introduction

The prostate gland is an accessory male reproductive organ below the bladder. It produces secretions that are integral parts of semen, which are necessary for sperm survival. In the adult male, the prostate gland is divided into three regions: Peripheral, central, and transitional. More than 95% of adenocarcinomas account for cases of prostate cancer, most arising in acinar cells, while a minority are traced back to ductal cells. More than 70% of the prostate's epithelial cells comprise the luminal or, in a few instances, basal cells at the peripheral zone, where 85% of prostate adenocarcinoma originates (Wasim et al., 2022).

Prostate cancer ranks second in incidence and fifth in terms of cancer-related mortality among males (Rawla, 2019). It is also the major cause of male cancer-associated deaths. Although considerable progress has been made in the diagnosis and treatment of prostate cancer, it remains a serious healthcare dilemma (Siegel et al., 2023). The incidence and death rates continue to rise, primarily due to its heterogeneous nature, which yields different prognoses, the lack of early detection markers, and the inefficiency of many lifetime therapies (Sung et al., 2021). Moreover, the unequal burdens and outcomes of the disease are frequently not similar between many racial groups (Yamoah et al., 2022; Chornokur et al., 2011). Prostate cancer diagnosis involves the use of prostate biopsy, analysis, digital rectal examination, Magnetic Resonance Imaging, Prostate-Specific Antigen, and health examinations. The risk of disease is age, weight, race, family history, and numerous environmental factors. Facts show that prostate cancer, as a disease, varies in genetic makeup and epidemiology. Further, differences in prostate cancer epidemiology between countries can be explained by the complex interplay between genetics, environmental variables, and societal factors; this leads to diverse survival rate estimates specific to each racial group (Hjelmborg et al., 2014).

Approximately 5% of men diagnosed with prostate cancer (PC) have distant metastases, often in multiple locations, while 15% present with locoregional metastases (Siegel et al., 2018). For those with late-stage PC (distant metastases), the overall five-year survival rate is only 30% (Siegel et al., 2018). PC metastasis causes over 400,000 deaths

* Corresponding Author.
Email Address: rmonshi@kau.edu.sa
https://doi.org/10.21833/ijaas.2025.12.008
Corresponding author's ORCID profile:
https://orcid.org/0000-0001-7696-0452

annually, with this mortality rate projected to at least double by 2040 (Sandhu et al., 2021). In addition, a similar proportion of males are anticipated to endure treatment-related morbidity for more than ten years after diagnosis (Sandhu et al., 2021). For extended periods, metastatic PC cells can lie latent in the tumor microenvironment in secondary sites. Over 80% of distant metastatic lesions in PC occur in bone tissue. The primary mechanisms of PC metastases include hematogenous spread to the bone marrow stroma in the axial skeleton and/or diffusion to locoregional lymph nodes (Berish et al., 2018).

In the early 1990s, the use of digital rectal exams (DRE) for prostate cancer screening resulted in a significant decrease in reported cases (Moradi et al., 2012). This exam not only helps differentiate between benign and malignant cells but also aids in detecting tumors in the posterior region of the prostate. However, its effectiveness in identifying tumors in other areas is limited. Prostate-specific antigen (PSA) screening, introduced in the same period, has shown promise in reducing mortality rates and complications, albeit with controversy (Skowronek, 2017). False-positive results and associated health issues, such as pain and infection, are common with PSA screening, particularly in asymptomatic individuals. Transrectal ultrasound (TRUS) under a systematic randomized method aids in detecting small and low-grade cancers but faces challenges due to its low sensitivity for large-scale screening (Park et al., 2016). Computer-aided design (CAD) methods offer diagnostic accuracy ranging from 0.80 to 0.89, with some studies reporting AUC values of 0.95 to 0.96 (Sarkar and Das, 2016). These systems often rely on manual candidate selection and data dependency. Ultrasound provides real-time imaging for initial detection but needs differentiation between cancerous and benign tissue. Yet, Multiparametric magnetic resonance imaging had higher tissue contrast than ultrasound, though to be used effectively, it requires extensive training and doesn't provide real-time imaging (Abbasi et al., 2020).

In recent years, the state of testicular cancer (TC) diagnosis and therapy has significantly improved. Depending on their performance, computer-aided diagnosis and prognostication assist surgeons in determining the health status of their patients using medical algorithms and apparatus (Wasim et al., 2022). CAD systems have been developed to serve either experts of decision support systems that evaluate medical and laboratory data and then provide practitioners with recommendations or perform additional activities such as assessing and interpreting a large variety of medical disorders (Ishioka et al., 2018). These systems are frequently used to identify irregularities and assist with interpreting and visualizing photographs such as X-rays, mammograms, CT scans, and MRIs, among others (Reda et al., 2016).

Systems that assist in CAD recognize specific features or patterns indicative of the presence of a disease or abnormality through machine learning, deep learning, and pattern recognition algorithms. They aid radiologists by highlighting regions of interest or providing quantitative measurements for further analysis. In decision-making, soft computing techniques play a vital role in a variety of medical image analysis fields. Deep learning, a form of AI, has a strong track record in pattern recognition and medical image classification (Aribisala and Olabanjo, 2018).

Prostate cancer detection is increasingly being facilitated by machine learning (ML) models that can analyze large datasets containing both medical records and imaging. These models help to analyze vast amounts of other types of information, including genetic data and histopathology reports. They can evaluate a person's risk of developing prostate cancer by examining all types of information, help to improve the accuracy of so-called PSA tests, analyze images of the male genital gland to identify abnormal growths, and determine the nature of the tumor and whether it is malignant. ML algorithms do not require the assistance of pathologists to analyze the latter and can detect cancer cells while making a prognosis for the patient. Furthermore, these models help oncologists create personalized treatment plans for patients by analyzing all types of information about them and suggesting the best strategies. The integration of ML-based detection with prostate cancer diagnostics increases accuracy in diagnosis as well as identifies patients early to initiate personally tailored treatment, thus promoting patient care and outcomes. This study is a step in this regard. The main contributions of this study are:

- An ensemble model is presented in this study for the accurate detection of prostate cancer. The ensemble model uses Xception, Inception-V3, and ResNet50 transfer learning models as base learners and finally predicts the class using the weighted ensemble approach.
- Voting and weighting ensemble approaches are evaluated using three models. Weighting ensembles performs much better than voting. Based on the results obtained from these models, 50% for the Xception model, 35% for Inception-v3, and 15% for ResNet50 are used.
- Keeping in view the small size of the dataset, the Conditional Generative Adversarial Network (CGAN) model is used to generate more samples. Experiments involve both the original dataset as well as the CGAN-based dataset for evaluation.

After the introduction, this paper is divided into five sections. In Section 2, related works are examined. The proposed approach is described in Section 3, along with the dataset, model building, performance metrics, and machine learning algorithms for classification. Section 4 presents and discusses the environmental setup, experimental outcome, and performance comparison. In conclusion, Section 5 offers a synopsis of this work,

summarizing the investigation and suggesting possible avenues for further research.

2. Literature review

Classification is a fundamental concept in machine learning and data mining, and it plays an important role in logical problem-solving, especially in medical applications such as prostate cancer (PC) detection. Sreenivasa et al. (2020) conducted a study in which they used machine learning models to detect both prostate and breast cancer. In their approach to reducing dimensionality, they applied several algorithms, including Decision Trees (DT), Random Forest (RF), Support Vector Machines (SVM), Naive Bayes (NB), and Logistic Regression (LR). Their results showed that LR achieved an accuracy of 91.25% on the prostate cancer dataset.

Similarly, Ozhan and Yagin (2022) proposed a machine learning system specifically designed to classify prostate cancer using clinical biomarkers. They developed a prediction model based on the RF algorithm and focused on risk factors such as area, perimeter, and texture. Their findings indicated that these features are important for distinguishing prostate cancer, and the RF model achieved an accuracy of 86%.

Recent advancements in artificial intelligence (AI), particularly in the realm of medical imaging and diagnosis, have opened transformative avenues for prostate cancer (PC) detection, classification, and management. In Haque et al. (2025), generative AI (GenAI) is explored as a revolutionary tool in prostate imaging. GenAI models, such as GANs, are increasingly used to generate synthetic medical images that mimic real patient scans, aiding in data augmentation, multi-modal imaging synthesis, and quality enhancement. The review outlines GenAI's role in digital pathology and classification of PC, while also discussing current limitations, including safety, clinical acceptance, and dataset diversity. Similarly, in a narrative review, Alis et al. (2025) focused on MRI-guided PC diagnosis. AI is shown to enhance diagnostic accuracy, reduce radiologist workload, and standardize interpretations. AI algorithms, especially those using deep learning, are effective in artifact detection, scan quality assessment, and lesion classification, achieving sensitivity comparable to that of expert radiologists. However, limitations in specificity and generalizability, due to dataset variability and methodological inconsistencies, still hinder wide clinical adoption.

Another research work, Arita et al. (2025), highlights the broader landscape of AI in PC management. Beyond diagnosis, AI tools are optimizing surgical skill assessments, predicting treatment outcomes, and enabling precision medicine. Machine learning models have demonstrated superior performance over conventional diagnostic methods in identifying clinically significant PC and personalizing care. Nevertheless, all reviews converge on the consensus that while AI offers immense potential, challenges such as small dataset sizes, lack of standardization, and clinical integration must be addressed to ensure robust and equitable deployment in real-world healthcare systems.

Srivenkatesh (2020) with an ML-based system for the effective prognosis of prostate cancer. Finally, a prediction model is presented to predict whether an individual has prostate cancer to help increase awareness and assist in diagnosis. SVM, RF, NB classifier, and LR are enumerated with popular ML algorithms, which are applied to data on the regions specifically of prostate cancer, and since the results of these rules are to be compared, predictors giving accurate machine learning models were chosen for the rule. In turn, it can be adduced that logistic regression and random forest have reasonable accuracy in comparison with other classifier ML algorithms, to 90% accuracy. Erdem and Bozkurt (2021) tested several machine learning and deep learning models for diagnosing prostate cancer. The models include k-nearest neighbors (kNN), Linear Discriminant Analysis (LDA), SVM, RF, Deep Neural Network (DNN), Multi-Layer Perceptrons (MLP), NB, Linear, and LR. Each of the methods is implemented more than ten times to avoid any vulnerabilities, since only five of the top ones were written down. The best accuracy of 97% and the lowest error of 0.03% were obtained in the case of MLP, according to the experimental results.

Laabidi and Aissaoui (2020) compared many well-known ML algorithms to find the most accurate predictive model for problems relating to medicine. Their results highlighted that the Recurrent Neural Network (RNN) produced the most balanced results, although Logistic Regression also performed exceptionally well, especially with scaled features. Hasan et al. (2021) utilized ML models and an ensemble learning approach for the effective prognosis of prostate cancer. They employed five linear models alongside an ensemble model for detecting prostate cancer. The study revealed that the ensemble model surpassed other individual learning models, achieving the highest accuracy score of 96.55%.

Mahadi et al. (2023) proposed a machine-learning-based framework to address the lack of specific guidelines for assessing prostate cancer indicators and the limited prognostic accuracy of current diagnostic methods. They applied several machine learning models and used GridSearch CV to optimize hyperparameters and improve classifier performance. Their approach achieved a very high accuracy of 96.67% for predicting the gender of Italian speakers using short speech samples.

Similarly, Saeedi et al. (2022) employed nine deep learning and machine learning models to identify fatal prostate cancer. Their modelling process was developed in the RapidMiner Studio environment. The results showed that the kNN and neural network models achieved an accuracy of 84%. Mezher et al. (2022) introduced an enhanced Genetic Folding (GF) model for prostate cancer

detection, achieving an impressive accuracy of 96%, currently the highest in prostate cancer diagnosis. Additionally, the GF model was applied to breast cancer classification with a suggested workflow. Gupta and Gupta (2022) conducted a thorough examination of cancer diagnosis at the data level, leveraging multiple cancer datasets. Their study revealed that the suggested stacked ensemble model attained a remarkable accuracy score of 97%.

Several trends in ML techniques for predicting cancer outcomes and susceptibility have been identified by a meta-analysis. The analysis revealed that an increasing array of machine learning techniques tends to enhance performance and prediction accuracy in prognosis, especially when contrasted with traditional statistical or expert-based systems. Advancements in experimental design and biological validation could significantly boost the overall quality and reproducibility of many machine-based classifiers. The summary of the discussed literature is given in Table 1.

3. Materials and methods

This section delves into the dataset used for detecting prostate cancer and describes the steps taken during data pre-processing. Additionally, it elaborates on the Transfer Learning models employed for prostate cancer prognosis.

3.1. Dataset

The ProstateX dataset, initially designed as a benchmark for prostate MRI analysis, has been superseded by the PI-CAI challenge, a comprehensive study incorporating over 10,000 curated prostate MRI exams (Litjens et al., 2017). This dataset was created to evaluate AI models for detecting and diagnosing clinically significant prostate cancer using MRI data. ProstateX-2 extended these efforts by focusing on the development of biomarkers from multi-parametric MRI to predict Gleason Grade Groups in prostate cancer. The dataset includes T2-weighted, proton density-weighted, dynamic contrast-enhanced, and diffusion-weighted imaging, acquired using Siemens MAGNETOM Trio and Skyra 3T MR scanners. These images were obtained through high-resolution sequences with specific acquisition parameters, including b-values for diffusion imaging, with ADC maps generated directly from scanner software. While ProstateX remains accessible for benchmarking purposes, its role has been integrated into the unified PI-CAI framework, which aims to standardize the clinical validation of prostate AI systems.

3.2. Generation of training data by CGAN

GANs are cutting-edge network models widely applied in unsupervised and semi-supervised learning. One component, generator G, produces synthetic data resembling real samples, while discriminator D assesses both real and synthetic data to distinguish between authentic and fabricated instances (Pan et al., 2019). These networks operate concurrently, aiming for a Nash equilibrium. Importantly, the generator lacks direct access to real data and interacts solely through the discriminator, which gauges authenticity. This process generates a ground truth-based error signal, refining the generator's output to create higher-quality synthetic data (Mirza and Osindero, 2014).

Table 1: Summary of the related work

Reference	Classifier	Performance
Sreenivasa et al. (2020)	DT, RF, SVM, NB, and LR	91.25% LR
Ozhan and Yagin (2022)	RF	86% RF
Srivenkatesh (2020)	SVM, RF, NB, LR, and kNN	90% LR and RF
Erdem and Bozkurt (2021)	kNN, SVM, RF, LR, Linear Regression, NB, LDA, Linear classification, MLP, and DNN	97% MLP
Laabidi and Aissaoui (2020)	XGB, RF, LR, DT, SVM, NB, kNN, and RNN	81.30% RNN
Hasan et al. (2021)	RF, SVM, kNN, LR, NN, and an ensemble model	96.55% Ensemble model
Mahadi et al. (2023)	SVC, LR, ADA, XGB, KNC, LGBM, GB, DT, and RF	96.67% XGB, LGBM, GB, and RF
Saeedi et al. (2022)	SVM, DT, NB, kNN, NN, RF, DL, Auto-MLP, and Rule induction algorithms	84% kNN, NN
Mezher et al. (2022)	Genetic Folding model (GF)	96% GF
Gupta and Gupta (2022)	DT, kNN, NB, GBC, XGB, and Stacked (RF+GBC+XGB)	97% Stacked (RF+GBC+XGB)

A network with multiple layers consisting of convolutional or fully connected layers is commonly employed as either a generator or a discriminator in GANs. The generator does not have to be entirely invertible; it only needs to be visible to the discriminator (Odena et al., 2017). Recent advancements in GAN technology have been detailed in several research studies. Several GAN approaches include fully connected GANs, convolutional GANs, conditional GANs, inference-model GANs, and adversarial autoencoder GANs (Chen et al., 2016). The subject of this study is conditional GANs, which have a conditional class for the discriminator and generator. Conditional variables are used by CGANs to improve multidimensional data production and control the random noise that was common in the first generation of GANs. Variants of CGANs, such as auxiliary GANs and InfoGANs, have also been proposed.

Each variant of CGAN has its advantages and disadvantages. This study suggests an improved CGAN that combines characteristics from earlier CGAN versions. It can be expressed mathematically as follows:

$$Lsource = [logP(S = Normal|XNormal)] + E[logP(S = Cancer|XCancer)] \quad (1)$$

$$Lclass = [logP(C = a|XNormal)] + E[logP(C = a|XCancer)] \quad (2)$$

$$I(a, G(na, a)) = Ex \sim G(n, a)[Ea \sim P(a|x)[logQ(a|x)]] + H(a) \quad (3)$$

Fig. 1 demonstrates the suggested enhanced CGAN. Three changes have been made to the current CGAN by the proposed CGAN.

- added a class or conditional variable to D,
- added a network extension using D, and
- Give a name to every data sample.

3.3. Transfer learning models

Transfer learning (TL) has shown considerable promise across different medical fields, such as predicting and diagnosing prostate cancer. TL algorithms are crucial for analyzing vast amounts of patient data, which helps in the early and accurate detection of potential prostate cancer cases. The effectiveness of TL models in predicting prostate cancer depends on the caliber and volume of data used during training. To create an accurate and dependable predictive model, one must have access to a wide range of representative datasets. This study utilizes ResNet-50, Inception V3, Xception, and their combination to explore prostate cancer detection and prediction.

Convolutional neural networks (CNNs) require large amounts of data to be trained. Manual annotation is required during the data acquisition process, which is labor- and time-intensive. The substantial computational resources required for network training pose challenges for many individuals. Transfer learning emerges as a viable solution to address the limitations posed by small sample datasets. Incremental parameter adjustments within a narrow range during training prove suitable for addressing the prostate cancer classification problem under investigation in this study. Hence, the advantage of transfer learning lies in its ability to bypass training a model from scratch, thereby saving significant training time and computational resources while achieving commendable performance on small sample datasets.

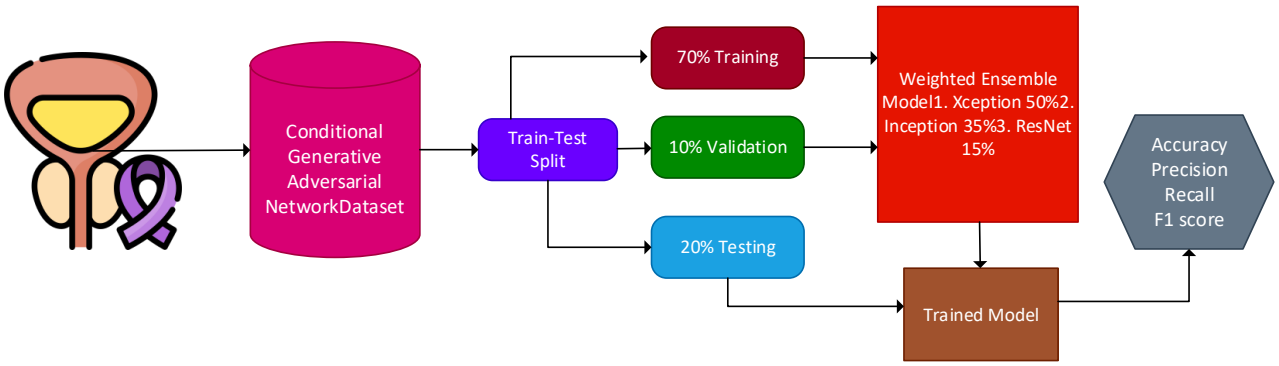

Fig. 1: The proposed model methodology

3.3.1. ResNet50

ResNet-50 represents a CNN variant with a depth of 50 layers, often chosen as a starting point for transfer learning tasks (Wang et al., 2019). Introduced by the Residual Network model, it pioneered the concept of skip connections. ResNet architecture is based on 5 stages; each stage consists of 3 CNN layers and blocks of identity. Due to this 5-stage architecture and CNN layers, ResNet 50 contains 23 million parameters to train the model accurately. The uniqueness of ResNet lies in getting the output of previous neurons to new layers to handle the vanishing gradient problem of deep CNN models.

3.3.2. Inception V3

Simply, Inception V3 was introduced as an improvement over the previous generation Inception architecture with a reduced computational requirement (Mujahid et al., 2022). This model is much more efficient in terms of memory usage and resource utilization as compared to the Google Net, Inception V1. The network uses various optimization methods for better adaptability of the model and to increase the overall performance. Factorized convolutions are one of the major reasons behind Inception V3's advantage, which reduces the number of weights in the network. This optimization enabled us to save some memory that would otherwise be utilized by the model for better accuracy. Within the Inception V3 network, grid size reduction for efficient feature extraction is carried out naturally using pooling operations. All these optimizations together make Inception V3 a very efficient and practical selection for use cases like prostate cancer detection, which involves both computational resources as well as model performance.

3.3.3. Xception

In 2017, Francois created an "Extreme Inception" that is Xception, an innovative deep learning architecture, referred to as Xception (Xtremely exceptional) (Salim et al., 2023). The novelty of Xception lies in its central block architecture, which is common in all previous models that are built on a

CNN baseline. The baseline CNN models utilized the input image for feature generation, while the Xception does the opposite and makes use of filter operations to extract significant features rather than complete input image features utilization. It uses depth-wise operations rather than pointwise as utilized in traditional CNNs. This technique is also useful to avoid overfitting during model training.

3.3.4. Ensemble

Because medical data has complex attributes and extracting features from it is difficult, a single learner's feature extraction ability is inherently limited, leading to challenges in achieving high-precision classification (Umer et al., 2022). Multiple basic learners are trained using ensemble learning, often known as the transfer learning strategy of" learning from others' strengths." After that, these learners are coupled with techniques to produce an ensemble model, which produces a strong learner. In addition to providing more stable, reliable, and accurate classification results, this technique guarantees variation in the extracted features, which helps to somewhat reduce overfitting. In our study, we utilized a transfer learning model that includes three different TL models: ResNet-50, Inception V3, and Xception.

3.3.5. Proposed ensemble learning model

For ensemble learning, two popular strategies are the weight-based ensemble and voting ensemble models. Let's say we have T learners denoted as $\{h_1, h_2, h_3, ..., h_T\}$. For a given prediction sample x, where the potential prediction categories are $\{c_1, c_2, ..., c_k\}$, and the prediction output of each learner is $\{h_1(x), h_2(x), ..., h_T(x)\}$, these strategies play a crucial role in combining the predictions effectively.

In this study, we employ three base learners: ResNet-50, Inception V3, and Xception. These base learners are utilized to obtain prediction results on prostate cancer samples to enhance the accuracy of the proposed model.

The weight ensemble approach is advised when there is a notable variation in the performance of individual models. This approach involves assigning a weight to each learner, and the ultimate prediction is calculated by averaging the weighted predictions of each learner.

$$TH(x) = \mathrm{X} wihi(x) \quad i = 1 \tag{4}$$

The i^{th} based learner's relevance is indicated by the weight w_i, which is determined via d_i. The value of d_i depends on the recognition accuracy of each base learner on the test set, sorted in ascending order. At d_i of 3, the base learner with the highest recognition rate is the highest performer, and at d_i of 1, the lowest performer.

In the voting ensemble method, the decision of the majority prevails. The final classification is determined by choosing the category with the highest number of votes from the predictions made by T learners on sample x. If there is a tie with multiple categories receiving the highest number of votes, one category is randomly chosen from them.

We performed initial experiments to analyze the efficacy of individual models, which showed that the ResNet50 performs poorly as an individual model. So, it is not advisable to use the soft voting method to make an ensemble of all transfer learning classifiers where some individual classifiers' performance is below the average. Considering that, we make a weighted voting ensemble of all transfer learning models by giving 50% weightage to the Xception model, 35% to Inception-v3, and 15% to ResNet50. The results obtained using this weighted voting classifier method are more accurate than the soft voting classification method.

3.4. Evaluation parameters

The performance of the classifier is assessed using many assessment measures in this study, including the F1 score, recall, accuracy, and precision. Accuracy compares the number of correctly classified samples over the total size of samples to determine how accurate the model's predictions are overall:

$$Accuracy = (TP + TN) / (TP + FP + TN + FN) \tag{5}$$

Recall assesses how well the classifier can recognize positive samples inside a given class.

$$Recall = TP / (TP + FN) \tag{6}$$

Precision calculates the proportion of all samples that were expected to be positive that were recognized as positive. The formula is used to calculate it:

$$Precision = TP / (TP + FP) \tag{7}$$

The F1 score is used in cases of data class imbalance, as it combines memory and precision into a single score:

$$F1\ score = 2 \times (Precision \times Recall) / (Precision + Recall) \tag{8}$$

4. Results and discussions

Extensive experiments were conducted for prostate cancer detection. Transfer learning models were applied for experiments. An ensemble of three individual transfer learning models was used for both datasets: the original dataset and the CGAN-generated dataset.

4.1. Experiment setup

The experiments were performed on a Python 3.8 programming environment. The setup includes

software libraries like Scikit-learn and TensorFlow. The rest of the details about the experimental setup and hyperparameters are shared in Table 2.

4.2. Result of transfer learning models on the original dataset

In the first phase of the experiment, individual transfer learning models are used on the original dataset. As the dataset has a low number of samples, the performance of the transfer learning models is poor. The result of the transfer learning model and the proposed transfer ensemble model is shown in Table 3. ResNet50 achieved an accuracy of 61%, with recall, precision, and F1-Score values of 62%, 68%, and 66% respectively. This indicates that while ResNet50 correctly classified a moderate percentage of instances, its precision suggests that a notable number of its positive predictions were correct. Inception-v3 demonstrated higher performance across all metrics compared to ResNet50, with an accuracy of 74% and balanced recall, precision, and F1 score of 74%, 75%, and 74% respectively. This implies that Inception-v3 is more accurate and balanced in its classification. Xception also showed competitive results with an accuracy of 73% and slightly lower recall, precision, and F1 scores of 72%, 73%, and 72% respectively. This suggests that Xception performed comparably to Inception-v3 but with a slightly lower recall rate. The ensemble model (soft) outperformed all individual models with an accuracy of 80% and balanced recall, precision, and F1 scores of 79%, 80%, and 80% respectively. The ensemble model, which combines predictions from multiple models, demonstrated the highest overall performance in terms of accuracy and balanced classification metrics.

However, the best performance is from the weighted ensemble model, which obtained 84.55% accuracy. Its precision, recall, and F1 scores are also better than all other models.

Table 2: Summary of experimental setup and hyperparameters

Parameter	Value
CGAN architecture	
Generator	4 ConvTranspose2D layers, ReLU, batch normalization, tanh
Discriminator	4 Conv2D layers, LeakyReLU (α = 0.2), dropout (0.4), sigmoid
Output image size	256 × 256 (grayscale)
Weight initialization	Xavier uniform
Loss function	Binary cross-entropy
Optimizer	Adam (lr = 0.0002, β1 = 0.5, β2 = 0.999)
Dropout rate	0.4 (in discriminator)
Epochs	12
Early stopping patience	3 epochs
Classifier training	ResNet50, InceptionV3, Xception
Classifier training settings	
Input size	256 × 256 × 3
Activation functions	ReLU (hidden), softmax (output)
Optimizer	Adam (lr = 0.001)
Batch size	32
Dropout rate	0.4
Dense layer units	256
Software and programming environment	
Language	Python 3.8
Libraries	TensorFlow, Scikit-learn, Keras, NumPy, Matplotlib
Operating system	Windows 11 (64-bit), beta build
Hardware specifications	
Processor	Intel Core i7-7700HQ @ 2.80 GHz (7th gen)
RAM	16 GB
GPU	NVIDIA GeForce GTX series (dedicated GPU)
Other settings	
Train split	70 (stratified)
Test split	20
Validation split	10
Data augmentation	Rotation (±15°), flip, crop (±10 px), brightness (0.9–1.1)
Framework	TensorFlow 2.10

Table 3: Classification results without using CGAN

Model	Accuracy	Recall	Precision	F1 score
ResNet50	61.17	62.67	68.42	66.53
Inception-v3	74.42	74.19	75.36	74.25
Xception	73.63	72.34	73.74	72.55
Ensemble (soft)	80.21	79.67	80.58	80.62
Ensemble (Weighted)	84.55	81.67	84.31	83.48

4.3. Result of transfer learning models with CGAN

In the second phase of the experiment, individual transfer learning models are used on the modified dataset using CGAN. By creating artificial data samples, the CGAN can help with the issue of limited data volume. The results of the transfer learning models and the proposed transfer ensemble model are shown in Table 4.

Table 4: Classification results using CGAN

Model	Accuracy	Recall	Precision	F1 score
ResNet50	73.39	75.64	78.96	77.72
Inception-v3	81.53	80.49	85.42	83.45
Xception	87.91	86.12	85.74	85.61
Ensemble (soft)	95.58	92.48	94.17	93.38
Ensemble (weighted)	98.25	96.75	97.58	96.65

The results of the ResNet50 model are noticeably improved, with an accuracy of 73% and improved recall, precision, and F1 scores of 75%, 78%, and 77% respectively. This enhancement suggests that integrating CGAN into the training process led to better classification results for ResNet50. For Inception-v3, the accuracy is increased to 81%, with higher recall, precision, and F1 score of 80%, 85%, and 83% respectively. It is an indication that the integration of CGAN had been improved for Inception-v3, hence, more precise and accurate classifications. Xception has significantly improved with accuracy at 87%, while recall and precision are now at 86% and 85%, with an F1 score amounting to 85%. What this simply means is that the ability of Xception to classify things accurately and more precisely is positively affected by using CGAN. The ensemble (soft) model improved substantially, and integration with CGAN advanced accuracy to an excellent 95%, together with improved recall, precision, and F1 scores reaching 92, 94, and 93%, respectively. It indicates that in this case, multiple models in conjunction with CGAN training led to accurate and highly precise classifications across the board. The best results are from the weighted ensemble model with a 98.25% accuracy, which is the best among all models. The smooth training of the proposed methodology is shared in Fig. 2.

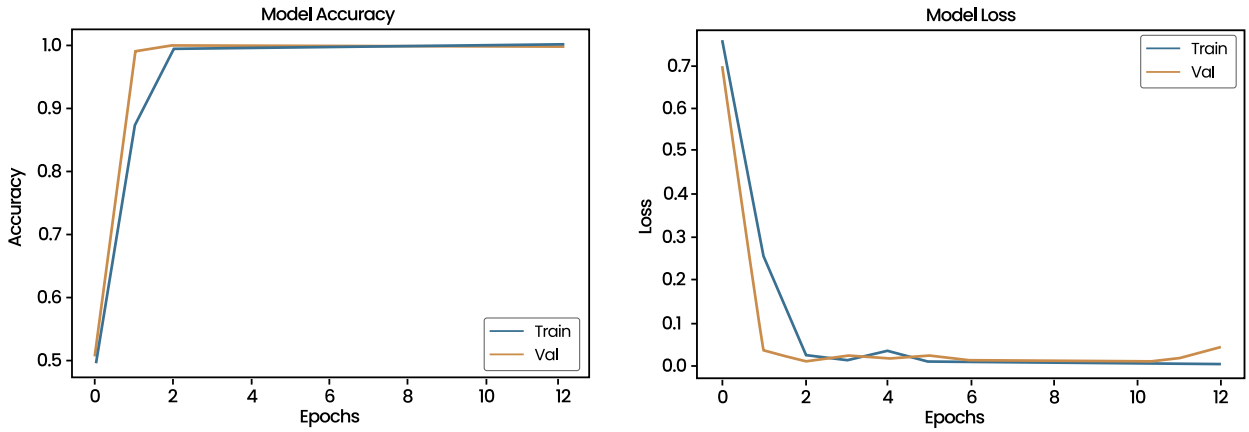

Fig. 2: Training accuracy and loss graph

4.4. Comparison of results with and without CGAN

In the training phase, the addition of a CGAN helped to significantly enhance the classification capabilities of the models examined. A comparison between the results without the CGAN and those with it revealed major improvements under every tested model, as shown in Table 5. Therefore, the overall accuracy of ResNet50 increased from 61% to 73%, showing a significant growth in the number of correctly classified instances. Moreover, the classifier of Inception-v3 showed significant improvements in the classifier's accuracy, from 74% up to as high as 81%, which suffices to prove that CGAN further boosted its classifying capabilities. Similarly, Xception reported an amazing rise in accuracy from 73% and reached 87%, which proves that the classifier was good enough with CGAN to keep such a high classification accuracy. The model achieved a fair performance with an 80% model accuracy without CGAN, though the inclusion of CGAN to the mix bumped this very considerably to a significant 95% accuracy. This very significant increase portrays immense value addition by the generative adversarial networks in the training process, especially for ensemble models to produce accurate and precise classifications.

Table 5: Classification results with and without the CGAN

Model	Without CGAN	With CGAN
ResNet50	61.17	73.39
Inception-v3	74.42	81.53
Xception	73.63	87.91
Ensemble (soft)	80.21	95.58
Ensemble (weighted)	84.55	98.25

4.5. Why is a weighted ensemble used?

Soft voting is another type of voting mechanism in which the result is the mean of the predicted probability values or score of the classifiers within the ensemble. This approach entails the following: integration of the probabilities of the classifiers, mean calculation of the said probabilities, and selection of a class label with the highest mean probability as the final prediction. The benefits associated with soft voting include mainly working well if the classifiers selected are well calibrated, preventing overfitting as the risk is spread out, and

being easy to implement and understand, which is not in this instance.

On the other hand, a weighted ensemble puts different weights on some of the classifiers depending on the performance of all the classifiers. The last prediction is commonly made using the weighted average of the probabilities (or the scores). This involves weighing the classifiers with certain coefficients, often their validation performances, then finding the weighted average of the probability estimates, and choosing the class label with the highest weighted average probability as the final decision. In a weighted ensemble, less accurate classifiers get a lower score than the more accurate classifiers; hence, if the overall strengths and weaknesses of various classifiers differ, this is an added advantage since it can be easily optimized to achieve the best outcome given different accuracies of various classifiers.

When making this decision, the following factors should be put into consideration: The soft voting method is appropriate where all the classifiers are of similar accuracy and calibration, or where model simplicity and interpretability are desirable. On the other hand, in cases where the classifiers' performances are significantly different, and you wish to capitalize on better performance, then a weighted ensemble is useful. This method is useful when weights can be quantified and adjusted with precision, since this implies that the relationships can be optimized. However, in practice, one can always try both ways and, based on cross-validation or a validation set, choose the better approach for the given situation.

4.6. Statistical significance testing

To validate the statistical significance of the performance improvement achieved by the proposed weighted ensemble method, we conducted paired t-tests against baseline and ensemble models using fivefold validation accuracy results. The results are shared in Table 6. The p-values for all comparisons were less than 0.05, indicating that the performance gains are statistically significant. This confirms that the improvement is not due to random variation and establishes the robustness of our approach.

Table 6: Paired t-test results comparing the weighted ensemble with other models

Model	T-statistic	P-value	Significant
ResNet50	131.9410	0.0001	Yes
Inception-v3	37.0734	0.0003	Yes
Xception	79.4827	0.0008	Yes

4.7. Results of cross-validation

K-fold cross-validation is used to make sure the models are reliable. Table 7 displays the 5-fold cross-validation results, which unequivocally show that the suggested strategy performs better than alternative models in terms of accuracy, recall, precision, and F1-score. The small standard deviation attests to the consideration of the method defined by its consistency and reliability. These results reveal that the recommended method consistently does well over various folds and that the method becomes more reliable and robust.

Table 7: Results using 5-fold cross-validation results using CGAN and a weighted voting classifier

	Accuracy	Recall	Precision	F1 score
1st fold	97.11	96.37	97.78	97.13
2nd fold	97.38	96.77	97.69	96.96
3rd fold	98.55	97.10	98.26	97.03
4th fold	98.02	97.18	98.42	97.09
5th fold	97.84	96.94	98.58	97.16
Average	97.78	96.87	98.14	97.07

4.8. Comparison with other models

To improve accuracy, a thorough investigation was done to evaluate the suggested model's performance against models from existing literature. Table 8 discusses some previously published work with the proposed model to judge the significance of the proposed model and thereby bring out its enhancements over the currently implemented practices.

This research is quite illuminating in the fact that the proposed model creates a higher enhancement accuracy in comparison to advanced models.

Table 8: Comparing performance with existing models

Reference	Approach	Accuracy
Sreenivasa et al. (2020)	LR	91.25%
Ozhan and Yagin (2022)	RF	86.01%
Srivenkatesh (2020)	LR and RF	90.13%
Erdem and Bozkurt (2021)	MLP	97.48%
Laabidi and Aissaoui (2020)	RNN	81.30%
Hasan et al. (2021)	Ensemble model	96.55%
Mahadi et al. (2023)	XGB, LGBM, GB, and RF	96.67%
Saeedi et al. (2022)	kNN, NN	84.74%
Mezher et al. (2022)	GF	96.11%
Gupta and Gupta (2022)	Stacked (RF+GBC+XGB)	97.04%
This study	Ensemble (ResNet50+ Inception-v3+ Xception)	98.25%

The suggested method demonstrates superior outcomes, particularly with small datasets. The improved performance of the ensemble mainly comes from the better performance of the Conditional Generative Adversarial Network, which compensates for the lack of data by generating synthetic samples. The model proposed in the work uses CGAN in the training procedure, purposely

constructed to overcome the drawbacks posed by discriminative models. However, there are some limitations to CGAN itself. One well-known drawback is that CGAN can generate good-quality data when the learned space maps the inputs. If the generator discovers a sample that easily deceives the discriminator, it may produce similar data, leading to training challenges and poor results when applied to unseen data instances.

4.9. Limitations and clinical relevance proposed framework

In this subsection, we critically analyze the key limitations of the proposed framework, including the limited diversity of the dataset, potential overfitting risks from CGAN-based data augmentation, and the absence of external clinical validation. We also acknowledge that while our model achieved high accuracy on internal and extended datasets, the true performance in a heterogeneous clinical environment may vary due to differences in imaging protocols, scanner quality, and patient demographics.

Additionally, we have elaborated on the clinical relevance of our proposed system by highlighting how it may assist radiologists in early diagnosis and reduce diagnostic subjectivity. We emphasize that the high precision and recall scores indicate potential for real-world applicability, especially in settings where rapid triage or second-opinion support is needed. However, we also clarify that before clinical deployment, the system must be rigorously tested on larger, multi-institutional datasets and validated through clinical trials.

4.10. Generalizability of the proposed framework

To evaluate the generalizability of the proposed CGAN-augmented weighted ensemble framework beyond the PROSTATEx dataset, additional experiments were conducted using a publicly available prostate MRI dataset provided by the National Cancer Institute (Bethesda, USA), collected between 2008 and 2010. The dataset comprises 22,036 MR images obtained from 26 participants, with a total of 182 series and 26 studies. Each image was acquired using a 3T Philips Achieva scanner with both endorectal and phased array surface coils. All patients had biopsy-confirmed prostate cancer and underwent robotic-assisted radical prostatectomy. A customized mold was used to align histopathology sections with imaging slices, ensuring spatial consistency and accurate ground truth labeling.

The proposed framework is evaluated on an external independent dataset without any additional fine-tuning to simulate a real-world deployment scenario. The goal was to assess the robustness and generalization capability of the model under distributional shifts due to imaging protocol variations, scanner differences, and subject diversity.

The evaluation results on the external dataset are summarized in Table 9. The model achieved an accuracy of 95.37%, a precision of 96.28%, a recall of 97.14%, and an F1-score of 96.86%. These high-performance scores demonstrate that the proposed ensemble framework retains strong predictive power even when applied to an independent dataset, supporting its robustness and potential for clinical applicability.

Table 9: Performance of the proposed model on the external prostate MRI dataset

Metric	Accuracy	Precision	Recall	F1-score
Value (%)	95.37	96.28	97.14	96.86

These findings confirm that the integration of CGAN-based data augmentation with a weighted ensemble of transfer learning models yields not only superior performance on internal test data but also demonstrates strong generalization across diverse clinical imaging datasets. This reinforces the framework's viability for broader deployment in real-world medical diagnostic workflows.

5. Conclusion

Prostate cancer is still a major health concern globally due to the non-symptomatic form that the disease manifests, especially in the beginning stages; hence, early diagnosis and treatment are rarely made. This study initiates a transfer learning-based method to improve the diagnosis of prostate cancer using the conditional generative adversarial network integrated with a weighted ensemble model. The models are weighted in the ensemble as ResNet (15%), Xception (50%), and Inception (35%), and experiments involved CGAN-based generated samples, as well as the original dataset. The weighted ensemble model proved to be the most effective due to its 98.25% accuracy, 96.75% precision, 97.58% recall, and 96.65% F-measure. Comparing the obtained results to the soft voting ensemble, it can be stated that the proposed model provides more reliable and accurate detection of prostate cancer. Furthermore, the comparative study with the present approaches from the literature and cross-validation reinforces the proposed approach. The findings of this study contribute to bettering the detection of prostate cancer; they demonstrate the possible directions in enhancing prostate cancer detection in the next studies and approaches for use in clinical practice.

List of abbreviations

ADC	Apparent diffusion coefficient
AI	Artificial intelligence
AUC	Area under the curve
CAD	Computer-aided diagnosis
CGAN	Conditional generative adversarial network
CNN	Convolutional neural network
CT	Computed tomography
DNN	Deep neural network
DRE	Digital rectal examination

DT	Decision tree
GB	Gradient boosting
GAN	Generative adversarial network
GF	Genetic folding
KNC	K-nearest centroid
kNN	K-nearest neighbors
LDA	Linear discriminant analysis
LGBM	Light gradient boosting machine
LR	Logistic regression
ML	Machine learning
MLP	Multi-layer perceptron
MRI	Magnetic resonance imaging
NB	Naïve Bayes
NN	Neural network
PC	Prostate cancer
PI-CAI	Prostate imaging – artificial intelligence
PSA	Prostate-specific antigen
ReLU	Rectified linear unit
RF	Random forest
RNN	Recurrent neural network
SVC	Support vector classifier
SVM	Support vector machine
TC	Testicular cancer
TL	Transfer learning
TRUS	Transrectal ultrasound
XGB	Extreme gradient boosting

Funding

This research work was funded by the Institutional Fund Projects under grant no. (IFPIP: 1446-415-1443). The author gratefully acknowledges the technical and financial support provided by the Ministry of Education and King Abdulaziz University, DSR, Jeddah, Saudi Arabia.

Compliance with ethical standards

Ethical considerations

The datasets used in this study (PROSTATEx and the National Cancer Institute prostate MRI dataset) are publicly available and fully anonymized. All patient identifiers were removed by the data providers prior to release. All procedures were performed in accordance with relevant guidelines and regulations.

Conflict of interest

The author(s) declared no potential conflicts of interest with respect to the research, authorship, and/or publication of this article.

References

Abbasi AA, Hussain L, Awan IA, Abbasi I, Majid A, Nadeem MSA, and Chaudhary QA (2020). Detecting prostate cancer using deep learning convolution neural network with transfer learning approach. Cognitive Neurodynamics, 14: 523–533. https://doi.org/10.1007/s11571-020-09587-5 **PMid:32655715 PMCid:PMC7334337**

Alis D, Onay A, Colak E, Karaarslan E, and Bakir B (2025). A narrative review of artificial intelligence in MRI-guided prostate cancer diagnosis: Addressing key challenges. Diagnostics, 15(11): 1342. https://doi.org/10.3390/diagnostics15111342 **PMid:40506914 PMCid:PMC12154491**

Aribisala BS and Olabanjo O (2018). Medical image processor and repository – MIPAR. Informatics in Medicine Unlocked, 12: 75–80. https://doi.org/10.1016/j.imu.2018.06.005

Arita Y, Roest C, Kwee TC et al. (2025). Advancements in artificial intelligence for prostate cancer: Optimizing diagnosis, treatment, and prognostic assessment. Asian Journal of Urology. https://doi.org/10.1016/j.ajur.2024.12.001

Berish RB, Ali AN, Telmer PG, Ronald JA, and Leong HS (2018). Translational models of prostate cancer bone metastasis. Nature Reviews Urology, 15(7): 403–421. https://doi.org/10.1038/s41585-018-0020-2 **PMid:29769644**

Chen X, Duan Y, Houthooft R, Schulman J, Sutskever I, and Abbeel P (2016). InfoGAN: Interpretable representation learning by information maximizing generative adversarial nets. In the Proceedings of Advances in Neural Information Processing Systems (NeurIPS), Barcelona, Spain: 2172–2180.

Chornokur G, Dalton K, Borysova ME, and Kumar NB (2011). Disparities at presentation, diagnosis, treatment, and survival in African American men, affected by prostate cancer. Prostate, 71(9): 985–997. https://doi.org/10.1002/pros.21314 **PMid:21541975 PMCid:PMC3083484**

Erdem E and Bozkurt F (2021). A comparison of various supervised machine learning techniques for prostate cancer prediction. Avrupa Bilim ve Teknoloji Dergisi, 21: 610–620.

Gupta S and Gupta M (2022). A comprehensive data-level investigation of cancer diagnosis on imbalanced data. Computational Intelligence, 38(1): 156–186. https://doi.org/10.1111/coin.12452

Haque F, Simon BD, Özyörük KB, Harmon SA, and Türkbey B (2025). Generative artificial intelligence in prostate cancer imaging. Balkan Medical Journal, 42(4): 286–300. https://doi.org/10.4274/balkanmedj.galenos.2025.2025-4-69 **PMid:40619793 PMCid:PMC12240228**

Hasan SM, Rabbi MF, and Jahan N (2021). Can machine learning technique predict the prostate cancer accurately? The fact and remedy. In the International Conference on Electronics, Communications and Information Technology (ICECIT), IEEE, Khulna, Bangladesh: 1-4. https://doi.org/10.1109/ICECIT54077.2021.9641099

Hjelmborg JB, Scheike T, Holst K et al. (2014). The heritability of prostate cancer in the Nordic Twin Study of Cancer. Cancer Epidemiology, Biomarkers & Prevention, 23(11): 2303–2310. https://doi.org/10.1158/1055-9965.EPI-13-0568 **PMid:24812039 PMCid:PMC4221420**

Ishioka J, Matsuoka Y, Uehara S et al. (2018). Computer-aided diagnosis of prostate cancer on magnetic resonance imaging using a convolutional neural network algorithm. BJU International, 122(3): 411–417. https://doi.org/10.1111/bju.14397 **PMid:29772101**

Laabidi A and Aissaoui M (2020). Performance analysis of machine learning classifiers for predicting diabetes and prostate cancer. In the 1st International Conference on Innovative Research in Applied Science, Engineering and Technology (IRASET), IEEE, Meknes, Morocco: 1-6. https://doi.org/10.1109/IRASET48871.2020.9092255

Litjens G, Debats O, Barentsz J, Karssemeijer N, and Huisman H (2017). SPIE-AAPM PROSTATEx challenge data (Version 2) [dataset]. The Cancer Imaging Archive. https://doi.org/10.7937/K9TCIA.2017.MURS5CL

Mahadi MK, Abir SR, Moon A et al. (2023). Machine learning assisted decision support system for prediction of prostate cancer. In the 20th International Conference on Electrical Engineering/Electronics, Computer, Telecommunications and Information Technology (ECTI-CON), IEEE, Nakhon Phanom,

Thailand: 1-5.
https://doi.org/10.1109/ECTI-CON58255.2023.10153167

Mezher MA, Altamimi A, and Altamimi R (2022). An enhanced genetic folding algorithm for prostate and breast cancer detection. PeerJ Computer Science, 8: e1015.
https://doi.org/10.7717/peerj-cs.1015
PMid:35875638 PMCid:PMC9299265

Mirza M and Osindero S (2014). Conditional generative adversarial nets. Arxiv Preprint Arxiv:1411.1784.
https://doi.org/10.48550/arXiv.1411.1784

Moradi M, Salcudean SE, Chang SD et al. (2012). Multiparametric MRI maps for detection and grading of dominant prostate tumors. Journal of Magnetic Resonance Imaging, 35(6): 1403–1413.
https://doi.org/10.1002/jmri.23540
PMid:22267089 PMCid:PMC5478377

Mujahid M, Rustam F, Álvarez R, Luis Vidal Mazón J, Díez ID, and Ashraf I (2022). Pneumonia classification from X-ray images with Inception-V3 and convolutional neural network. Diagnostics, 12(5): 1280.
https://doi.org/10.3390/diagnostics12051280
PMid:35626436 PMCid:PMC9140837

Odena A, Olah C, and Shlens J (2017). Conditional image synthesis with auxiliary classifier GANs. In the Proceedings of the 34th International Conference on Machine Learning, PMLR, Sydney, Australia, 70: 2642–2651.

Ozhan O and Yagin FH (2022). Machine learning approach for classification of prostate cancer based on clinical biomarkers. The Journal of Cognitive Systems, 7(2): 17–20.
https://doi.org/10.52876/jcs.1221425

Pan Z, Yu W, Yi X, Khan A, Yuan F, and Zheng Y (2019). Recent progress on generative adversarial networks (GANs): A survey. IEEE Access, 7: 36322–36333.
https://doi.org/10.1109/ACCESS.2019.2905015

Park JK, Kwon BK, Park JH, and Kang DJ (2016). Machine learning-based imaging system for surface defect inspection. International Journal of Precision Engineering and Manufacturing-Green Technology, 3: 303–310.
https://doi.org/10.1007/s40684-016-0039-x

Rawla P (2019). Epidemiology of prostate cancer. World Journal of Oncology, 10(2): 63–89.
https://doi.org/10.14740/wjon1191
PMid:31068988 PMCid:PMC6497009

Reda I, Shalaby A, Abou El-Ghar M et al. (2016). A new NMF-autoencoder based CAD system for early diagnosis of prostate cancer. In the IEEE 13th International Symposium on Biomedical Imaging (ISBI), IEEE, Prague, Czech Republic: 1237-1240. https://doi.org/10.1109/ISBI.2016.7493490

Saeedi S, Maghooli K, Amirazodi S, and Rezayi S (2022). Towards a better diagnosis of prostate cancer: Application of machine learning algorithms. Frontiers in Health Informatics, 11: 116.
https://doi.org/10.30699/fhi.v11i1.382

Salim F, Saeed F, Basurra S, Qasem SN, and Al-Hadhrami T (2023). DenseNet-201 and Xception pre-trained deep learning models for fruit recognition. Electronics, 12(14): 3132.
https://doi.org/10.3390/electronics12143132

Sandhu S, Moore CM, Chiong E, Beltran H, Bristow RG, and Williams SG (2021). Prostate cancer. The Lancet, 398(10305): 1075–1090.
https://doi.org/10.1016/S0140-6736(21)00950-8
PMid:34370973

Sarkar S and Das S (2016). A review of imaging methods for prostate cancer detection: Supplementary issue: Image and video acquisition and processing for clinical applications. Biomedical Engineering and Computational Biology, 7: BECB.S34255.
https://doi.org/10.4137/BECB.S34255
PMid:26966397 PMCid:PMC4777886

Siegel RL, Miller KD, and Jemal A (2018). Cancer statistics, 2018. CA: A Cancer Journal for Clinicians, 68(1): 7–30.
https://doi.org/10.3322/caac.21442 **PMid:29313949**

Siegel RL, Miller KD, Wagle NS, and Jemal A (2023). Cancer statistics, 2023. CA: A Cancer Journal for Clinicians, 73(1): 17–48. https://doi.org/10.3322/caac.21763 **PMid:36633525**

Skowronek J (2017). Current status of brachytherapy in cancer treatment–Short overview. Journal of Contemporary Brachytherapy, 9(6): 581–589.
https://doi.org/10.5114/jcb.2017.72607
PMid:29441104 PMCid:PMC5808003

Sreenivasa BC, Agrawal P, Deb S, Shilpa AV, and Raju SNR (2020). Breast cancer and prostate cancer detection using classification algorithms. International Journal of Engineering Research & Technology (IJERT), 9(6): 40–46.
https://doi.org/10.17577/IJERTV9IS060085

Srivenkatesh M (2020). Prediction of prostate cancer using machine learning algorithms. International Journal of Recent Technology and Engineering, 8(5): 5353–5362.
https://doi.org/10.35940/ijrte.E6754.018520

Sung H, Ferlay J, Siegel RL, Laversanne M, Soerjomataram I, Jemal A, and Bray F (2021). Global cancer statistics 2020: GLOBOCAN estimates of incidence and mortality worldwide for 36 cancers in 185 countries. CA: A Cancer Journal for Clinicians, 71(3): 209–249.
https://doi.org/10.3322/caac.21660 **PMid:33538338**

Umer M, Naveed M, Alrowais F et al. (2022). Breast cancer detection using convoluted features and ensemble machine learning algorithm. Cancers, 14(23): 6015.
https://doi.org/10.3390/cancers14236015
PMid:36497497 PMCid:PMC9737339

Wang ZY, Xia QM, Yan JW, Xuan SQ, Su JH, and Yang CF (2019). Hyperspectral image classification based on spectral and spatial information using multi-scale ResNet. Applied Sciences, 9(22): 4890. https://doi.org/10.3390/app9224890

Wasim S, Lee S, and Kim J (2022). Complexities of prostate cancer. International Journal of Molecular Sciences, 23(22): 14257.
https://doi.org/10.3390/ijms232214257
PMid:36430730 PMCid:PMC9696501

Yamoah K, Lee KM, Awasthi S et al. (2022). Racial and ethnic disparities in prostate cancer outcomes in the Veterans Affairs health care system. JAMA Network Open, 5(1): e2144027.
https://doi.org/10.1001/jamanetworkopen.2021.44027
PMid:35040965 PMCid:PMC8767437